



Modulation format identification under stringent bandwidth limitation based on an artificial neural network

LUYAO HUANG, LEI XUE, QUNBI ZHUGE,  WEISHENG HU,  AND LILIN YI*

State Key Lab of Advanced Optical Communication Systems and Networks, Shanghai Institute for Advanced Communication and Data Science, Shanghai Jiao Tong University, Shanghai 200240, China
*lilinyi@sjtu.edu.cn

Abstract: A new method based on an artificial neural network (ANN) and asynchronous amplitude histograms (AAHs) is designed for modulation formats identification (MFI) in a bandwidth-limited intensity modulation direct detection (IM/DD) system. The proposed method recognizes modulation format features of AAHs and the signal is extracted before equalization algorithms such as FFE and CMA for limited bandwidth and chromatic dispersion (CD). Three IM/DD modulation formats, non-return-to-zero (NRZ), 4-level pulse amplitude modulation (PAM4), and 8-level pulse amplitude modulation (PAM8) are recognized. The numerical simulation results manifest that MFI accuracy can reach up to 95% with a 30-40% bandwidth limitation. Furthermore, we evaluate the effectiveness of the method in the experiment, and 100% identification accuracy can be achieved even when the system is under 36.76% bandwidth limitation. The proposed method is implemented in DSP without extra hardware and is promising for optical performance monitoring in next-generation elastic optical networks (EONs).

© 2021 Optical Society of America under the terms of the [OSA Open Access Publishing Agreement](#)

1. Introduction

Driven by the fast and large-scale information exchange in data center traffic, 5G mobile optical front-haul and back-haul systems, and various cases, channel capacity continues to grow exponentially in the optical communication system. Such traffic growth places massive demands on a dynamic and transparent network architecture with reconfigurable optical add-drop multiplexers (ROADMs), flexible grid, and advanced modulation formats. The construction of such a dynamic optical network such as elastic optical networks (EONs) highly depends on the precise estimation of channels and signals information. Therefore, a comprehensive and sophisticated optical performance monitoring (OPM) system needs to be implemented across the whole link. Among versatile OPM parameters such as optical power, data rate, optical signal noise ratio (OSNR) [1–5], chromatic dispersion (CD) [6–7], polarization-mode dispersion (PMD), fiber nonlinearity, etc., modulation format is the most fundamental one. Because the symbol decision and decoding in the receiver side should first know the modulation format information, some digital OSNR estimation methods based on statistical features [8–10] also need the knowledge of modulation format, and some equalization algorithms like least mean square (LMS) are not transparent for modulation format, therefore, how to achieve precise MFI is the research focus.

There have been many demonstrations proposed for MFI, such as the k-means algorithm [11], RF-pilot aided method [12], Stokes parameters [13–14], support vector machine (SVM) [15], and random forest [16]. Out of these techniques, the machine learning (ML)-based MFI subsystem is the most versatile and promising. Neural network (NN), which contains a variety of variants, is the most typical one among many ML techniques. The simplest one is artificial neural networks (ANN), whose layers are fully connected [17–20]. Other network architectures such as

convolutional neural networks (CNN) [21–24] and recurrent neural network (RNN) especially long short-term memory (LSTM) [25–26] are also explored. Several parameters can be utilized as input for NN, such as asynchronous amplitude histograms (AAHs), asynchronous delay-tap plots (ADTP) [27], and Stokes parameters [28]. In this work, ANN with AAH is chosen for its lowest complexity and good performance.

Most MFI techniques are deployed in coherent communication system and recognize modulation formats such as quadrature phase-shift keying (QPSK), 16-level quadrature amplitude modulation (16QAM), and 64-level quadrature amplitude modulation (64QAM), but its application in intensity modulation direct detection (IM/DD) system is also necessary. In [19], three typical modulation formats recognition in IM/DD system are demonstrated, but the problem of bandwidth limit is not considered, and an additional CMA equalization algorithm is required before NN. Low cost is a universal requirement in IM/DD system. To save the deployment cost, utilizing low complexity or removing equalization algorithms and reusing the legacy devices with limited bandwidth are preferred in IM/DD systems. The relationship between bandwidth limitation and recognition accuracy is worth studying and the degradation boundary needs to be found.

In this paper, we propose an ANN-based MFI method to identify three typical modulation formats in a bandwidth limitation IM/DD transmission system by both simulation and experimental demonstration, including non-return-to-zero (NRZ), 4-level pulse amplitude modulation (PAM4), and 8-level pulse amplitude modulation (PAM8). We focus on the identification accuracy of 20 Gbaud and 50 Gbaud signals after transmission in a bandwidth-limited system. This method is tolerant to CD and bandwidth limit, thus the signal used for MFI is not compensated by any DSP algorithm. In the simulation, the ANN-based MFI method can achieve a high recognition rate (>95%) with a 30%-40% band limit. In the experiment, 20 Gbaud signals are transmitted with 20-km fiber and MFI accuracy of 100% for the three modulation formats is achieved until 4G bandwidth limitation and degradation boundary is 35.21% bandwidth of the signal, which matches with the simulation results. The remainder of this paper is organized as follows. In section 2, we describe the configuration of AAH and ANN. In section 3, a numerical simulation analysis is given to verify the effectiveness of the ANN-based MFI method. Bandwidth limitation filter is used to emulate low-cost and low bandwidth receiver. Finally, we experiment to further indicate the practicability of our method in section 4.

2. Configuration of AAH and ANN

AAHs with 50 bins are generated after fiber transmission and bandwidth limitation filter and before the equalization algorithm. Our choice of recognizing modulation format at an earlier stage of the DSP chain is based on the following reasons. MFI is not only indispensable for symbol decision at the transmission end points but also intermediate network nodes. OPM devices implemented at these points are required to use low-cost and low bandwidth receiver and have simple hardware construction to achieve real-time processing. By estimating modulation format before the feed-forward equalizer (FFE), our proposed approach requires only a few DSP blocks, thus the DSP complexity of OPM devices can be reduced partially. The AAHs for three 50 Gbaud modulation formats under two different circumstances are considered in this work as shown in Fig. 1(a). Without equalization, signal in the optical system is degraded by serious linear impairment such as chromatic dispersion (CD) and device bandwidth limitation. As we can see, the AAHs of signal with different modulation formats exhibit distinct patterns after CD compensation. However, if CD is not compensated, it's hard to distinguish formats by eyes. CD compensation can be implemented in simulation and we ignore the CD distortions for better AAH presentation. But in our communication system, due to PD direct detection, the received signal only has intensity information and phase information is lost. It's difficult to compensate CD completely in DSP. Therefore, more powerful data analysis methods should be applied to extract modulation format sensitive features of AAHs without any DSP such as FFE.

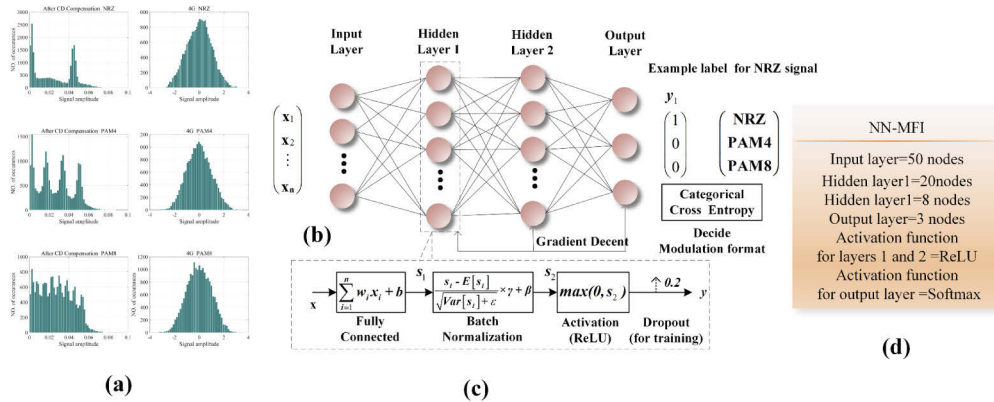


Fig. 1. The structure and parameters of AAHs and ANN in the simulation and experiment set up. (a) AAHs of NRZ, PAM4, and PAM8 with 50 bins of 50 GBaud signal after CD compensation and 4G bandwidth-limited receiver. (b) NN structure. (c) Flow chart for the hidden layer. (d) Network parameters.

Figure 1(b) shows the structure of the proposed ANN for MFI. ANN is written by Python based on the TensorFlow framework. It is a 4-layer network, containing two hidden layers. The circles denote the nodes. The input layer has 50 nodes equal to AAH’s bin numbers. The output layer has 3 nodes. After Softmax and Argmax function, if the output vector is $[1,0,0]$, NN classifies the signal’s modulation format is NRZ. Similarly, $[0,1,0]$ means PAM4 and $[0,0,1]$ means PAM8.

Other important network parameters and functions of ANNs used in this work are given in Fig. 1(d), which is customized for our identification. The network is trained with backpropagation and gradient descent with Adam optimization. The cross-entropy loss of output will be back-propagated to update the weight parameters by mini-batch gradient descent with the batch size of 16. Meantime, Adam will adaptively adjust the learning rate depending on the first and second-order moment estimation, to increase the training efficiency, and accelerate the convergent speed. Batch normalization is added to avoid gradient explosion and accelerate network training speed. In the case of overfitting, dropout strategy with the dropout rate of 0.2 is employed.

AAH dataset for training and test are generated corresponding to three modulation formats. Every 10,000 symbols are grouped to obtain one 50 bins AAH. After training, ANN’s performance will be evaluated by test samples, usually, 30% of the whole data set, and picked up randomly. The network parameter is fixed after training and the modulation format is predicted by output vector. The MFI information provided by ANN-MFI is then utilized to select the optimized demodulation scheme.

3. Simulation setup and results

Matlab is used to simulate this IMDD system shown in Fig. 2(a). Transmitted data is 20/50-Gbaud NRZ, PAM4, and PAM8 signal with a length of 1,000,000. The reason that different modulation formats with the same baud rate rather than bit rate are adopted is that we prefer these signals occupying identical channel bandwidth and at the receiver side they are under identical bandwidth limitation, which is prone to compare. The rooted raised cosine (RRC) filter together with the matched filter is used to eliminate inter-symbol interference. An ideal MZM is added to convert the electrical signal to an optical signal. Note that the MZM is chosen here because we focus on the relationship between MFI accuracy and system bandwidth. The modulator with chirp effects will be tested in the following experiment. After the optical transmitter, an erbium-doped fiber amplifier (EDFA) is used to amplify the signal and simultaneously introduce amplified

spontaneous emission (ASE) noise with a 5-dB noise figure. The Split-step Fourier method is extensively used to solve the pulse-propagation problem in nonlinear dispersive media and we use this numerical technique to simulate dispersion and nonlinear effect in optical fiber. Fiber length is 80 km, and other parameters are the same as the standard single-mode fiber (SSMF) presented in Fig. 2(b). After fiber transmission and photo-diode (PD) detection, the received data stream is filtered by an exponential lowpass filter served as bandwidth limitation, whose frequency response and the transfer function is shown in Fig. 2(e). In the transfer function, m is filter order and f_L is the expected bandwidth limit. The later data stream is sent into the DSP model for MFI and equalization. The occurrence number at each bin is selected as input features for the following ANN. 100 AAHs for each format and there are 300 samples for the total dataset, 210 for training, and 90 for the test. Dataset is small but sufficient.

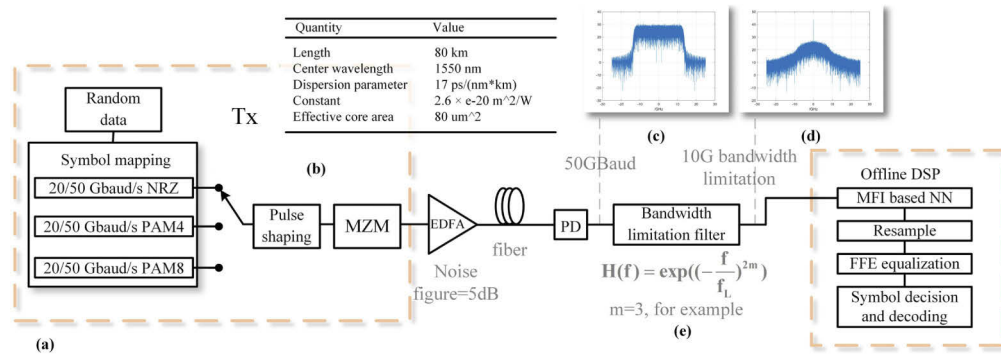


Fig. 2. (a) Simulation setup for 20/50-Gbaud NRZ/PAM4/PAM8 MFI system under bandwidth limitation. (b) Fiber parameter table. (c) The electrical spectrum of 50 GBaud signal. (d) The electrical spectrum of 10G bandwidth limited signal. (e) The transfer function of the bandwidth limitation filter.

First, we conduct MFI of 50 GBaud PAM4 signal without CD compensation and bandwidth limitation. The training and test accuracy can reach up to 100%. However, CD compensation algorithms are always required before MFI of QAM signal shown in [29–30]. We consider that NN is more efficient to process the real signal. When dealing with the complex signal in a coherent system, the real part and imaginary part are separated as two closed inputs. Without fine training, it is hard for NN to emulate the frequency domain and realize MFI at the same time. Thus, it's difficult for a single NN to achieve the same performance as a conventional equalization algorithm combined with NN. PAM formats only contain intensity information, it's easy for NN to emulate the FFE algorithm therefore no CD algorithm is needed before MFI.

Symbol error rate (SER) is adopted to evaluate signal quality before and after FFE. Figure 3(c) shows the relationship between receiver bandwidth and SER when the signal is transmitted at 50 GBaud rate. Dotted curves represent SER before FFE and solid curves after FFE. Curves of SER for three formats before FFE remain high and stable, which shows channel impairment degrades the signal's quality greatly and significant bandwidth reduction can't deteriorate the signal anymore. Curves after FFE also remain high with narrow bandwidth but decrease with the increase of bandwidth since FFE is used to equalize band-limited channels. OSNR of signals is also presented in Fig. 3(d) and (f). We utilize received signal distribution and error vector magnitude (EVM) [31] to estimate OSNR [32]. This estimation method is accurate if the received optical field is perturbed by AWGN only. Since launch power is 0dbm, fiber nonlinearity is trivial and the channel only has linear impairments. After FFE linear impairments are mitigated. So in Fig. 3(d) and (f), solid curves show accurate OSNR, and dotted curves are presented signal's all impairment only as a reference. In this OSNR estimation approach, r_k is the k_{th} received

symbol and can be represented as

$$r_k = s_k + n'_k = s_k + n_k + d_k, \quad (1)$$

where s_k is the transmitted symbol and n_k is the k^{th} of noise vectors. $n'_k = n_k + d_k$ consists of ASE noise n_k and linearity-induced distortions d_k . We propose OSNR through

$$\text{OSNR}_{\text{estimated}} = \frac{P_{in}}{P_{ASE} + P_{distortion}} = E \left(\frac{|s_k|^2}{|n'_k|^2} \right), \quad (2)$$

where P_{in} is the signal power, P_{ASE} represents the noise power, $P_{distortion}$ is linear and nonlinear distortions power and $E(\cdot)$ denotes expectation calculation. Figure 3(a) shows a graphical illustration of distributions of fully equalized signal and amplitude noise. The optical signal can be expressed like this since except amplitude light has another degree of freedom, phase. In the electric field, a coherent received signal also has two dimensions and contains phase information. Signal adopting advanced modulation format such as QAM is suitable for Fig. 3(a). As for the IMDD system, signal is received by the square-law photodetector, so the corresponding graphic is one dimension shown in Fig. 3(b).

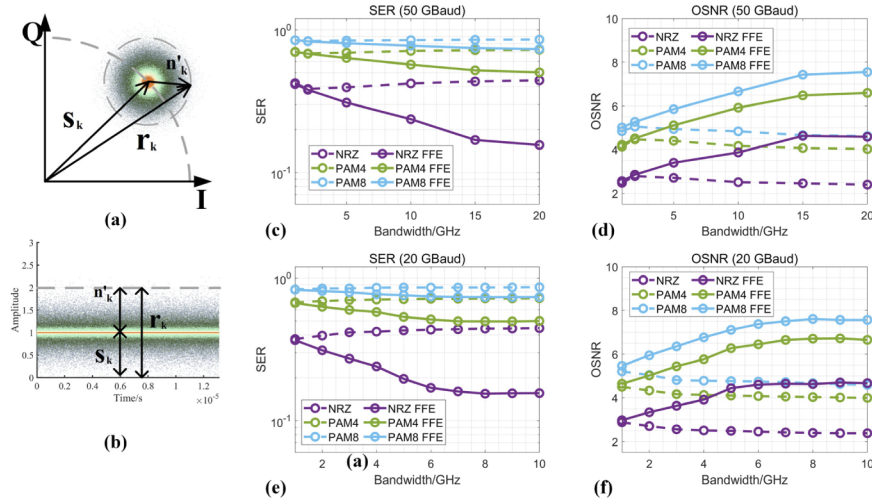


Fig. 3. Illustration of OSNR calculation process and SER and OSNR for simulation signal. (a) One of the symbols in simulated constellation diagram with Gaussian noise. (b) One of the levels in simulated one dimension signal's time domain diagram with Gaussian noise. (c) SER and (d) OSNR for 50 GBaud signal. (e) SER and (f) OSNR for 20 GBaud signal.

As depicted in Fig. 3(d), the signal impairment ratio of 50 GBaud rate signal before FFE remains low and stable which is consistent with SER. OSNR after FFE increases steadily from 1G band-limit to 15G band-limit and remains stable after 15G band-limit which matches with SER. Signal quality deteriorates sharply with a narrow bandwidth receiver. SER and OSNR of 20 GBaud rate signals are exhibited in Fig. 3(e) and (f). The SERs are larger than 0.1 and OSNRs are lower than 8dB. Both charts manifest bandwidth-limited signal's inferior quality.

Even signal is degraded by such severe linear distortion and most of the signal's information is lost, format information can still be extracted by ANN. Figure 4(a) shows the training and test accuracy of 50 GBaud signals. As we can see the training accuracy is 100% all the time. The test accuracy is 100% at 20 GHz and 15 GHz bandwidth, and 96.63% and 87.64% at 10G and 5G respectively. Test accuracy declines slightly between 15 GHz and 5 GHz and drops rapidly with

a bandwidth smaller than 5 GHz. MFI based ANN method can achieve a high recognition rate (>95%) with a 40% bandwidth limit. Figure 4(b) presents MFI accuracy of 20 GBaud signals and indicates that ANN can realize 100% test accuracy with a 30% bandwidth limit, which is similar but better than the former case. We conclude ANN can perform high recognition accuracy under a 30-40% bandwidth limit.

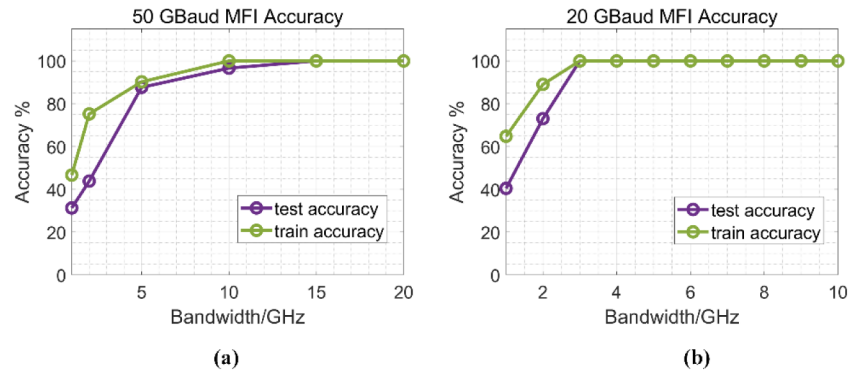


Fig. 4. MFI train and test accuracy in the simulation system. (a) accuracy results of 50GBaud signal. (b) accuracy results of 20GBaud signal.

4. Experiment setup and results

In the above simulation, the effectiveness of ANN-based MFI in the BW-limit system is verified. To verify the practicability of our method in a real deployment, we conduct an experiment in a bandwidth limited IMDD system. The experimental setup is demonstrated in Fig. 5. A Keysight M8195A AWG with a 65 GSa/s sampling rate generates 20-GBaud NRZ/PAM4/PAM8 random sequence. The signal from AWG is directly modulated by a 1550 nm directly-modulated laser (DML). An EDFA is followed by the DML to control the launch optical power. Fiber length is 20km, which is shorter than the simulation but within the PON field's coverage. After SSMF transmission, a variable optical attenuator (VOA) regarded as the splitter is used to adjust the power of the received signal. Another EDFA is utilized as a preamplifier in ONU to input suitable optical power of the 10/20G-class PD without a trans-impedance amplifier (TIA). The 3-dB bandwidth of the whole system is 13.6 GHz and 14.2 GHz respectively. The received electrical signal is amplified by an electrical amplifier (EA) and sampled by a LeCroy oscilloscope (DSO) with a 30 GHz bandwidth and 80 GSa/s sample rate. The Signal's electrical spectrum before and after the bandwidth limitation filter is shown in Fig. 5(b) and (c). Then digital signals are sent into the proposed offline DSP.

ANN structure, optimization algorithm, and the procedure of data organizing for ANN input are the same as simulation. SERs and OSNRs for 10G PD receiver are shown in Fig. 6(a) and (b), where all SERs are higher than 0.05, presenting poor signal quality. As for the test accuracy of MFI shown in Fig. 6(c), it is 100% from 5G to 10G bandwidth limit and drops slightly with lower than 5G. Test accuracy for the 4G bandwidth limit is 93.26%, which is a little smaller than 95%. The bandwidth limit is 36.76% to guarantee high MFI accuracy. For bandwidth-limited signal, the SERs, OSNRs, and MFI accuracy after 20-km transmission are plotted in Fig. 6(e)-(g). Test accuracy shows a minimal drop at the 4G bandwidth limit. The bandwidth limit is 35.21%, which is better than 10G PD at B2B. This is because though the signal is transmitted through fiber, the system 3-dB frequency response is to a small degree wider than 10G PD, which counteracts a part of fiber impairment. Figure 6(d) and (h) show training and validation costs every 10 iterations for B2B and fiber with 2G bandwidth-limit, which indicates our NN is neither overfitting nor

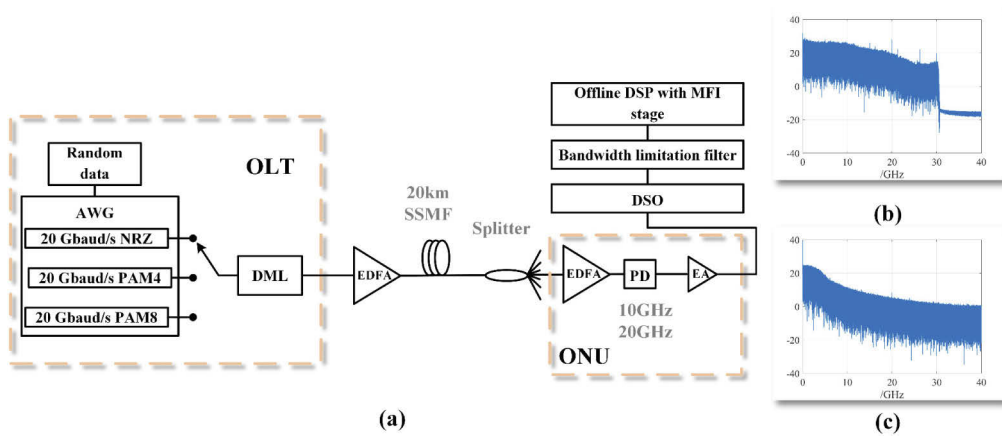


Fig. 5. (a) Experiment setup for 20/50-Gbaud/s NRZ/PAM4/PAM8 system under bandwidth limitation. (b) The electrical spectrum of a signal. (c) The electrical spectrum of 5G bandwidth limited signal.

underfitting. These experiment results match with numerical results and confirm the validity of our MFI method under stringent bandwidth limitation.

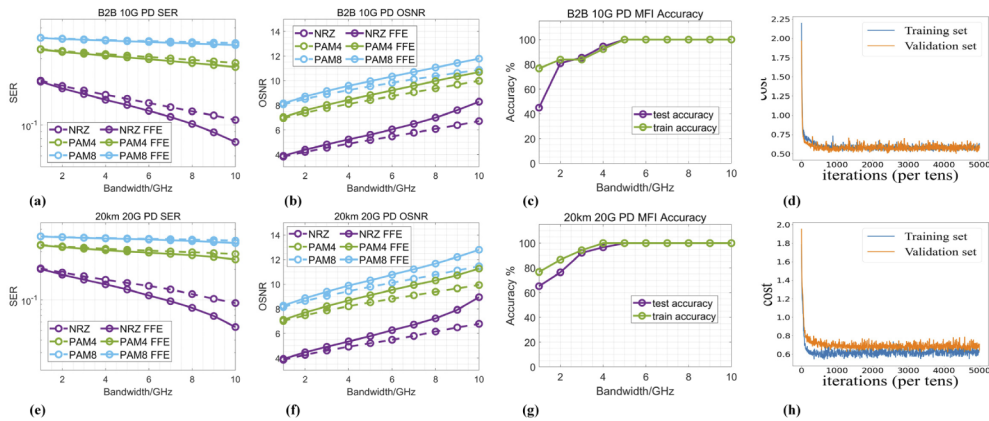


Fig. 6. (a) SER, (b) OSNR, and (c) training and test accuracy of 20 GBaud signals with 10G PD without fiber transmission, (e) SER, (f) OSNR, and (g) training and test accuracy of 20 GBaud signals with 20G PD and 20 km fiber transmission, Training and validation costs for (d) B2B and (h) fiber with 2G bandwidth-limit.

5. Conclusion

We successfully demonstrate a low cost MFI method based on AHH and ANN for NRZ, PAM4, and PAM8 signal under bandwidth limitation and impairment of CD in IM/DD system. We use SER and OSNR to measure signal quality. SER and OSNR curves present the same tendency and both manifest abysmal quality of the signal. Our method achieves 100% test accuracy for 50 GBaud signals from none to 10G limit and 20 GBaud signals from none to the 3G limit in simulation. The degradation boundary is 30-40% band limit. In the experiment, MFI for 10G PD B2B signal and 20G PD with 20km fiber transmission is investigated. Accuracy deterioration begins at 5 GHz for both and bandwidth limit ratios are 36.76% and 35.21%. MFI information

in IM/DD system is significant and beneficial for further OSNR estimation. OSNR and other parameters estimation under the bandwidth limit is worth further investigation.

Funding. National Key Research and Development Program of China (2019YFB1803803).

Disclosures. The authors declare no conflicts of interest.

References

1. F. N. Khan, K. Zhong, X. Zhou, W. H. Al-Arashi, C. Yu, C. Lu, and A. P. T. Lau, "Joint OSNR monitoring and modulation format identification in digital coherent receivers using deep neural networks," *Opt. Express* **25**(15), 17767–17776 (2017).
2. F. N. Khan, Y. Yu, M. C. Tan, W. H. Al-Arashi, C. Yu, A. P. T. Lau, and C. Lu, "Experimental demonstration of joint OSNR monitoring and modulation format identification using asynchronous single channel sampling," *Opt. Express* **23**(23), 30337–30346 (2015).
3. M. M. Feres, C. Floridia, and M. A. Romero, "Optimisation algorithms for OSNR measurement based on polarisation nulling," *Electron. Lett.* **51**(13), 1007–1009 (2015).
4. T. S. R. Shen, Q. Sui, and A. P. T. Lau, "OSNR Monitoring for PM-QPSK Systems with Large Inline Chromatic Dispersion Using Artificial Neural Network Technique," *IEEE Photonics Technol. Lett.* **24**(17), 1564–1567 (2012).
5. L. Xia, J. Zhang, S. Hu, M. Zhu, Y. Song, and K. Qiu, "Transfer learning assisted deep neural network for OSNR estimation," *Opt. Express* **27**(14), 19398–19406 (2019).
6. Q. Sui, A. P. T. Lau, and C. Lu, "Fast and robust blind chromatic dispersion estimation using auto-correlation of signal power waveform for digital coherent systems," *J. Lightwave Technol.* **31**(2), 306–312 (2013).
7. C. Wang, S. Fu, H. Wu, M. Luo, X. Li, M. Tang, and D. Liu, "Joint OSNR and CD monitoring in digital coherent receiver using long short-term memory neural network," *Opt. Express* **27**(5), 6936–6945 (2019).
8. R. Schmogrow, B. Nebendahl, M. Winter, A. Josten, D. Hillerkuss, S. Koenig, J. Meyer, M. Dreschmann, M. Huebner, C. Koos, J. Becker, W. Freude, and J. Leuthold, "Error vector magnitude as a performance measure for advanced modulation formats," *IEEE Photonics Technol. Lett.* **24**(1), 61–63 (2012).
9. C. Zhu, An V. Tran, S. Chen, L. B. Du, C. C. Do, T. Anderson, A. J. Lowery, and E. Skafidas, "Statistical moments-based OSNR monitoring for coherent optical systems," *Opt. Express* **20**(16), 17711–17721 (2012).
10. X. Lin, O. A. Dobre, T. M. N. Ngatched, and C. Li, "A Non-Data-Aided OSNR estimation algorithm for coherent optical fiber communication systems employing multilevel constellations," *J. Lightwave Technol.* **37**(15), 3815–3825 (2019).
11. N. G. Gonzalez, D. Zibar, and I. T. Monroy, "Cognitive digital receiver for burst mode phase modulated radio over fiber links," in *Proc. European Conference and Exhibition on Optical Communication (ECOC'2010)*, paper P.6.11.
12. M. Xiang, Q. Zhuge, M. Qiu, X. Zhou, M. Tang, D. Liu, S. Fu, and D. V. Plant, "RF-pilot aided modulation format identification for hitless coherent transceiver," *Opt. Express* **25**(1), 463–471 (2017).
13. R. Borkowski, D. Zibar, A. Caballero, V. Arlunno, and I. T. Monroy, "Stokes Space-Based Optical Modulation Format Recognition for Digital Coherent Receivers," *IEEE Photonics Technol. Lett.* **25**(21), 2129–2132 (2013).
14. L. Jiang, L. Yan, A. Yi, Y. Pan, T. Bo, and M. Hao, "Blind Density-Peak-Based Modulation Format Identification for Elastic Optical Networks," *J. Lightwave Technol.* **36**(14), 2850–2858 (2018).
15. X. Lin, O. A. Dobre, T. M. N. Ngatched, Y. A. Eldemerdash, and C. Li, "Joint modulation classification and OSNR estimation enabled by support vector machine," *IEEE Photonics Technol. Lett.* **30**(24), 2127–2130 (2018).
16. Y. Zhao, C. Shi, D. Wang, X. Chen, L. Wang, T. Yang, and J. Du, "Low-Complexity and nonlinearity-tolerant modulation format identification using random forest," *IEEE Photonics Technol. Lett.* **31**(11), 853–856 (2019).
17. A. Yi, L. Yan, H. Liu, L. Jiang, Y. Pan, B. Luo, and W. Pan, "Modulation format identification and OSNR monitoring using density distributions in Stokes axes for digital coherent receivers," *Opt. Express* **27**(4), 4471–4479 (2019).
18. F. N. Khan, Y. Zhou, A. P. T. Lau, and C. Lu, "Modulation format identification in heterogeneous fiber-optic networks using artificial neural networks," *Opt. Express* **20**(11), 12422–12431 (2012).
19. Z. Wan, Z. Yu, L. Shu, Y. Zhao, H. Zhang, and K. Xu, "Intelligent optical performance monitor using multi-task learning based artificial neural network," *Opt. Express* **27**(8), 11281–11291 (2019).
20. Y. Cheng, S. Fu, M. Tang, and D. Liu, "Multi-task deep neural network (MT-DNN) enabled optical performance monitoring from directly detected PDM-QAM signals," *Opt. Express* **27**(13), 19062–19074 (2019).
21. D. Wang, M. Zhang, Z. Li, J. Li, M. Fu, Y. Cui, X. Chen, D. Wang, M. Zhang, and Z. Li, "Modulation Format Recognition and OSNR Estimation Using CNN-Based Deep Learning," *IEEE Photonics Technol. Lett.* **29**(19), 1667–1670 (2017).
22. D. Wang, M. Wang, M. Zhang, Z. Zhang, H. Yang, J. Li, J. Li, and X. Chen, "Cost-effective and data size-adaptive OPM at intermediated node using convolutional neural network-based image processor," *Opt. Express* **27**(7), 9403–9419 (2019).
23. T. Tanimura, T. Hoshida, T. Kato, S. Watanabe, and H. Morikawa, "Convolutional Neural Network-Based Optical Performance Monitoring for Optical Transport Networks," *J. Opt. Commun. Netw.* **11**(1), A52–A59 (2019).
24. X. Fan, Y. Xie, F. Ren, Y. Zhang, X. Huang, W. Chen, T. Zhangsun, and J. Wang, "Joint Optical Performance Monitoring and Modulation Format/Bit-Rate Identification by CNN-Based Multi-Task Learning," *IEEE Photonics J.* **10**(5), 1–12 (2018).

25. Z. Wang, A. Yang, P. Guo, and P. He, "OSNR and nonlinear noise power estimation for optical fiber communication systems using LSTM based deep learning technique," *Opt. Express* **26**(16), 21346–21357 (2018).
26. C. Wang, S. Fu, Z. Xiao, M. Tang, and D. Liu, "Long Short-Term Memory Neural Network (LSTM-NN) Enabled Accurate Optical Signal-to-Noise Ratio (OSNR) Monitoring," *J. Lightwave Technol.* **37**(16), 4140–4146 (2019).
27. J. Zhou and P. Fan, "Modulation format/bit rate recognition based on principal component analysis (PCA) and artificial neural networks (ANNs)," *OSA Continuum* **2**(3), 923–937 (2019).
28. W. Zhang, D. Zhu, Z. He, N. Zhang, X. Zhang, H. Zhang, and Y. Li, "Identifying modulation formats through 2D Stokes planes with deep neural networks," *Opt. Express* **26**(18), 23507–23517 (2018).
29. J. Liu, Z. Dong, K. Zhong, A. P. T. Lau, C. Lu, and Y. Lu, "Modulation format identification based on received signal power distributions for digital coherent receivers," in *Proc. Optical Fiber Communication Conference (OFC'2014)*, paper Th2A.29.
30. F. N. Khan, K. Zhong, W. H. Al-Arashi, C. Yu, C. Lu, and A. P. T. Lau, "Modulation format identification in coherent receivers using deep machine learning," *IEEE Photonics Technol. Lett.* **28**(17), 1886–1889 (2016).
31. R. Schmogrow, B. Nebendahl, M. Winter, A. Josten, D. Hillerkuss, S. Koenig, J. Meyer, M. Dreschmann, M. Huebner, C. Koos, J. Becker, W. Freude, and J. Leuthold, "Error vector magnitude as a performance measure for advanced modulation formats," *IEEE Photonics Technol. Lett.* **24**(1), 61–63 (2012).
32. Z. Dong, A. P. T. Lau, and C. Lu, "OSNR monitoring for QPSK and 16-QAM systems in presence of fiber nonlinearities for digital coherent receivers," *Opt. Express* **20**(17), 19520–19534 (2012).